Inorg. Chem. **2008**, *47*, 3815−3822

Fluxional Behavior of Platinum(0) Complexes: Intra vs Intermolecular Reaction Pathways

Olena V. Zenkina,[†] Leonid Konstantinovski,[‡] Dalia Freeman,[†] Linda J. W. Shimon,[‡] and Milko E. van der Boom*,[†]

Department of Organic Chemistry and Department of Chemical Research Support, Weizmann Institute of Science, 76100 Rehovot, Israel

Received December 17, 2007

The fluxional behavior of two analogous platinum complexes has been studied in solution by NMR spectroscopy to elucidate the reaction mechanism and to determine the activation parameters. This includes variable temperature NMR spectroscopy, 2D $^1H-^1H$ exchange spectroscopy, and spin saturation transfer measurements. A platinum moiety, $Pt(PEt_3)_2$, translocates between two carbon−carbon double bonds of two vinylpyridine moieties bridged by an arene (i.e., phenyl, anthracene) at elevated temperatures. Magnetization transfer NMR experiments in the presence of free ligands unambiguously revealed an intramolecular pathway for the "phenyl" system. An intermolecular pathway is proposed for the "anthracene" complex.

Introduction

Arene complexes are thought to be intermediates in many metal-mediated transformations, including synthetically important carbon−carbon coupling reactions.[1–6] Studying and understanding the fluxional behavior of transition-metal complexes, including metal−arene interactions, is rarely an easy task.[7–30] Intermediates tend to be short-lived and occur in minute concentrations. η^2-Arene coordination to a metal center is much weaker than η^2-olefin coordination; one likely rationale for this is the loss of aromaticity. The crystal structures of an anthracene-nickel complex and related systems provided direct evidence for room temperature η^2-coordination of an aromatic hydrocarbon to a transition metal.[20] Similar interactions have been observed with (per) fluorinated aromatic systems and are known to be involved

* To whom correspondence should be addressed. E-mail: milko.vanderboom@weizmann.ac.il.
† Department of Organic Chemistry.
‡ Department of Chemical Research Support.

(1) Astruc, D. *Modern Arene Chemistry: Concepts, Synthesis, and Applications*; Wiley: New York, 2002.
(2) Kündig, P. *New aspects of transition metal arene complexes in organic synthesis*; Springer: New York, 2004; Topics in Organometallic Chemistry, Vol. 7.
(3) Crabtree, R. H. *The Organometallic Chemistry of the Transition Metals*, 4th ed.; Wiley: New York, 2005.
(4) Collman, J. P.; Hegedus, L. S.; Norton, J. R.; Finke, R. G. *Principles of Organotransition Metal Chemistry*, 2nd ed.; University Science Books: Oxford, 2006.
(5) Diederich, F.; Stang, P. J. *Metal catalyzed cross-coupling reactions*; Wiley-VCH: New York, 1998.
(6) van der Boom, M. E.; Milstein, D. *Chem. Rev.* **2003**, *103*, 1759.
(7) O'Connor, J. M.; Casey, C. P. *Chem. Rev.* **1987**, *87*, 307.
(8) Bach, I.; Pörschke, K.-R.; Goddard, R.; Kopiske, C.; Krüger, C.; Rufińska, A.; Seevogel, K. *Organometallics* **1996**, *15*, 4959.
(9) Sweet, J. R.; Graham, W. A. G. *Organometallics* **1983**, *2*, 135.
(10) Stanger, A.; Vollhardt, K. P. C. *Organometallics* **1992**, *11*, 317.
(11) Siegel, J. S.; Baldridge, K. K.; Linden, A.; Dorta, R. *J. Am. Chem. Soc.* **2006**, *128*, 10644.
(12) Schuster-Woldan, H. G.; Basolo, F. *J. Am. Chem. Soc.* **1966**, *88*, 1657.
(13) Zingales, F.; Chiesa, A.; Basolo, F. *J. Am. Chem. Soc.* **1966**, *88*, 2707.
(14) Strawser, D.; Karton, A.; Zenkina, O. V.; Iron, M. A.; Shimon, L. J. W.; Martin, J. M. L.; van der Boom, M. E. *J. Am. Chem. Soc.* **2005**, *127*, 9322.
(15) Zenkina, O.; Altman, M.; Leitus, G.; Shimon, L. J. W.; Cohen, R.; van der Boom, M. E. *Organometallics* **2007**, *26*, 4528.
(16) Zenkina, O. V.; Karton, A.; Freeman, D.; Shimon, L. J. W.; Martin, J. M. L.; van der Boom, M. E. *Inorg. Chem.* **2008**, in press.
(17) Iverson, C. N.; Lachicotte, R. J.; Müller, C.; Jones, W. D. *Organometallics* **2002**, *21*, 5320.
(18) Carbo, J. J.; Eisenstein, O.; Higgitt, C. L.; Klahn, A. H.; Maseras, F.; Oelckers, B.; Perutz, R. N. *Dalton Trans.* **2001**, 1452.
(19) Cotton, F. A. *Acc. Chem. Res.* **1968**, *1*, 257.
(20) Brauer, D. J.; Kruger, C. *Inorg. Chem.* **1977**, *16*, 884.
(21) Stanger, A.; Weismann, H. *J. Organomet. Chem.* **1996**, *515*, 183.
(22) Stanger, A.; Boese, R. *J. Organomet. Chem.* **1992**, *430*, 235.
(23) Stanger, A. *Organometallics* **1991**, *10*, 2979.
(24) Boese, R.; Stanger, A.; Stellberg, P.; Shazar, A. *Angew. Chem., Int. Ed. Engl.* **1993**, *32*, 1475.
(25) Cadenbach, T.; Gemel, C.; Schmid, R.; Fischer, R. A. *J. Am. Chem. Soc.* **2005**, *127*, 17068.
(26) Top, S.; Vessieres, A.; Jaouen, G.; Fish, R. H. *Organometallics* **2006**, *25*, 3293.
(27) Perthuisot, C.; Jones, W. D. *New J. Chem.* **1994**, *18*, 621.
(28) Hubig, S. M.; Lindeman, S. V.; Kochi, J. K. *Coord. Chem. Rev.* **2000**, *200–202*, 831.
(29) Jordan, M.; Saak, W.; Haase, D.; Beckhaus, R. *Eur. J. Inorg. Chem.* **2007**, 5168.
(30) Harman, W. D. *Chem. Rev.* **1997**, *97*, 1953.

10.1021/ic702433s CCC: $40.75 © 2008 American Chemical Society
Published on Web 03/28/2008

Scheme 1. Two Examples of Metal−Arene Complexes in which the Metal Center Migrates via an Intramolecular Pathway over the Aromatic Systems[10,11,21,23]

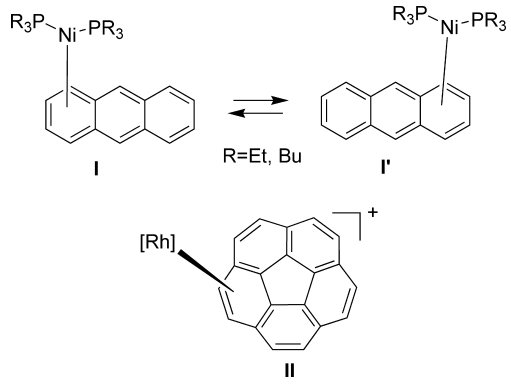

in aryl−F bond activation.[18,31] Interestingly, the first studies on reaction pathways involving metal−arene interactions were already carried out in the 1960s by the late Fred Basolo.[12,13] Other examples include the intramolecular migration of a $(R_3P)_2Ni$ (R = Et, Bu) moiety over an anthracene ligand via a series of $\eta^2-\eta^3$ haptotropic rearrangements along the system's outer carbon−carbon double bonds (Scheme 1, **I** ⇄ **I′**),[10,21,23] and the fluxional behavior of a d^8 rhodium corannulene complex (**II**).[11] Siegel, Baldridge, and Dorta reported recently that a metal center can even migrate over the curved aromatic surface of a corannulene ligand (**II**) without metal–ligand dissociation.[11] In addition to numerous experimental studies,[7–30] metal−arene interactions have been studied extensively using various computational methods.[14–16,18,31–35]

We reported very recently that the reaction of $Ni(PEt_3)_4$ with a halogenated vinyl-arene results in η^2-C═C coordination of $Ni(PEt_3)_2$, followed by "ring-walking" of the metal center to yield the thermodynamically favorable product of aryl-halide oxidative addition (Scheme 2, **III** → **IV**).[16] Similar processes were observed earlier by us with $Pt(PEt_3)_2$ using halogenated vinyl-arenes and azobenzene-derivatives.[15] However, the aryl-halide bond activation step was found to be rate determining with platinum,[14,15] thus making it difficult to obtain detailed information about the preceding processes. Intramolecular reaction pathways have been used to direct a metal center to a specific aryl-bond,[15–17,36,37] making it even possible to activate relatively strong aryl−Br bonds in the presence of substrates containing much weaker aryl−I bonds (e.g., compare Bond Dissociation Energy

Scheme 2. Examples of Reactions in which "Ring Walking" Processes are Coupled with Arene Functionalization[14–16]

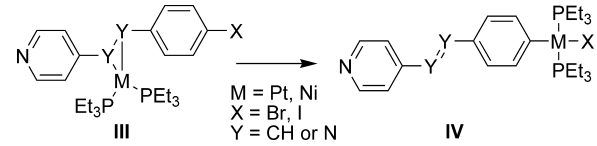

(BDE), Ph−Br = 80.5 kcal/mol vs Ph−I = 65.5 kcal/mol).[38] "Ring-walking" coupled with C−halide activation has synthetic utility, as demonstrated by Yokozawa et al.[39–41] They demonstrated that nickel-catalyzed chain growth polymerization of poly(p-phenylene) and poly(3-hexylthiophene) proceeds by intramolecular transfer of the Ni(0) catalyst, followed by selective cleavage of only one of the C−Br bonds. Furthermore, Harman et al. reported arene functionalization by means of various intramolecular structural rearrangements with a series of osmium complexes.[42,43] Interestingly, metal−substrate interactions coupled with bond activation/formation are not limited to arenes and thiophenes; a metal center can even bind to aliphatic hydrocarbons and "walk" along the chain before activation of a C−H bond.[44,45]

Intramolecular processes involving metal−arene interactions are especially interesting when mechanistic details can be obtained. In this report, we replaced the halide (X = Br, I) in the platinum stilbazole system (Scheme 2, **III**, Y = CH) with a vinylpyridine moiety in order to eliminate the irreversible formation of complex **IV**. This allows the metal center to migrate between the two C═C bonds linked via an arene in a reversible manner. This process has been studied here in solution by NMR spectroscopy to elucidate the underlying reaction mechanism and reaction parameters. This includes variable temperature (VT) NMR spectroscopy, 2D $^1H-^1H$ exchange spectroscopy (EXSY), and spin saturation transfer (SST) measurements. Furthermore, the intramolecular nature of the "ring walking" process has been demonstrated by SST experiments in the presence of free ligand.

Experimental Section

Materials and Methods. All reactions were carried out in a N_2-filled M. Braun glovebox with H_2O and O_2 levels <2 ppm. Solvents were reagent grade or better, dried, distilled, and degassed before being introduced into the glovebox, where they were stored over activated 4 Å molecular sieves. Deuterated solvents were purchased from Aldrich and were degassed and stored over 4 Å activated molecular sieves in the glovebox. Reaction flasks were washed with deionized (DI) water, followed by acetone, and then oven-dried at 130 °C prior to use. Mass-spectrometry was carried out using a

(31) Higgit, C. L.; Klahn, A. H.; Moore, M. H.; Oelckers, B.; Partridge, M. G.; Perutz, R. N. J. C. S. *Dalton Trans.* **1997**, 1269.
(32) Cohen, R.; Weitz, E.; Martin, J. M. L.; Ratner, M. A. *Organometallics* **2004**, *23*, 2315.
(33) Reinhold, M.; McGrady, J. E.; Perutz, R. N. *J. Am. Chem. Soc.* **2004**, *126*, 5268.
(34) Stępien, M.; Latos-Grażyñski, L.; Szterenberg, L.; Panek, J.; Latajka, Z. *J. Am. Chem. Soc.* **2004**, *126*, 4566.
(35) Di Bella, S.; Lanza, G.; Fragalà, I. L.; Marks, T. J. *Organometallics* **1996**, *15*, 3985.
(36) Slagt, M. Q.; Rodriguez, G.; Grutters, M. M. P.; Gebbink, R. J. M. K.; Klopper, W.; Jenneskens, L. W.; Lutz, M.; Spek, A. L.; van Koten, G. *Chem.—Eur. J.* **2004**, *10*, 1331.
(37) Rodriguez, G.; Albrecht, M.; Schoenmaker, J.; Ford, A.; Lutz, M.; Spek, A. L.; van Koten, G. *J. Am. Chem. Soc.* **2002**, *124*, 5127.
(38) *CRC Handbook of Chemistry and Physics*, 83rd ed.; Lide, D. R., Ed.; CRC Press: Boca Raton, FL, 2002–2003.
(39) Miyakoshi, R.; Yokoyama, A.; Yokozawa, T. *J. Am. Chem. Soc.* **2005**, *127*, 17542.
(40) Miyakoshi, R.; Shimono, K.; Yokoyama, A.; Yokozawa, T. *J. Am. Chem. Soc.* **2006**, *128*, 128.
(41) Yokoyama, A.; Yokozawa, T. *Macromolecules* **2007**, *40*, 4093.
(42) Harman, W. D. *Coord. Chem. Rev.* **2004**, *248*, 853.
(43) Keane, J. M.; Harman, W. D. *Organometallics* **2005**, *24*, 1786.
(44) Northcutt, T. O.; Wick, D. D.; Vetter, A. J.; Jones, W. D. *J. Am. Chem. Soc.* **2001**, *123*, 7257.
(45) Stahl, S. S.; Labinger, J. A.; Bercaw, J. E. *J. Am. Chem. Soc.* **1996**, *118*, 5961.

Micromass Platform LCZ 4000 system. Elemental analyses were performed by H. Kolbe, Mikroanalytisches Laboratorium, Mülheim an der Ruhr, Germany. Ligands **1**, **4**, and $Pt(PEt_3)_4$ were prepared by published procedures.[46–49]

Spectroscopic Analysis. The ^1H, $^{13}C\{^1H\}$, and $^{31}P\{^1H\}$ NMR spectra were recorded at 400.19, 100.6, and 161.9 MHz, respectively, on a Bruker Avance 400 NMR spectrometer. The $^{195}Pt\{^1H\}$ NMR spectra were recorded at 107.04 MHz on a Bruker Avance 500 NMR spectrometer. All chemical shifts (δ) are reported in ppm and coupling constants (J) in Hz. The ^1H and $^{13}C\{^1H\}$ NMR chemical shifts are relative to tetramethylsilane; the resonance of the residual protons of the solvent was used as the internal standard (7.15 ppm, benzene; 7.09 ppm, toluene; 6.95 and 2.20 ppm, *o*-xylene, 3.58 ppm, and 1.73 ppm, tetrahydrofuran) and all *d*-solvent peaks (128.0 ppm, benzene; 20.4 ppm, toluene; 19.6 ppm, *o*-xylene, tetrahydrofuran 67.6 ppm, and 25.3 ppm), respectively. $^{31}P\{^1H\}$ NMR chemical shifts are relative to 85% H_3PO_4 in D_2O (external reference), with shifts downfield of the reference considered positive. All measurements were carried out at 298 K unless otherwise stated. Screw-cap 5-mm tubes were used in NMR follow-up experiments. Vacuum/pressure valve 5-mm NMR sample tubes were used for all VT and magnetization transfer experiments. Assignments of the ^1H and $^{13}C\{^1H\}$ NMR spectra were made using gs-COSY, $^1H\{^{31}P\}$, and ^{13}C-DEPT-135 NMR experiments. VT ^1H NMR spectra were recorded on a Bruker Avance 400 NMR spectrometer in *o*-xylene-d_{10} at temperatures ranging from 183 to 393 K. Temperature calibration of the spectrometer was performed using CH_3OH/CD_3OD (<279 K) and $HOCH_2CH_2OH/d_6$-DMSO (>298 K). Temperature accuracy of the VT experiments was ± 0.2 °C. All 2D spectra (COSY, gs-NOESY) were acquired in the phase-sensitive mode. All data was acquired, processed, and displayed using Bruker XWinNMR software and a standard pulse-sequence library.

Formation of Complex 2. A solution of $Pt(PEt_3)_4$ (59 mg, 0.088 mmol) in 5 mL of dry tetrahydrofuran (THF) was dropwise added to a solution of bis-1,4-(4-pyridylethyl-enyl)-benzene (**1**)[46,48,49] (25 mg, 0.088 mmol) in 5 mL of dry THF and stirred at room temperature for 15 min. Removal of all volatiles in vacuo and washing of the residue with ~3 mL of dry pentane afforded the analytically pure complex **2** as a yellow solid in 85% yield. ^1H NMR (*o*-xylene-d_{10}): δ 8.64–8.69 (A part of AB system, 2H, PyrH, J_{HH} = 6.3 Hz), 8.51–8.47 (B part of AB system, 2H, PyrH, J_{HH} = 5.9 Hz), 7.39 (d, 2H, ArH, J_{HH} = 4.5 Hz), 7.27 (d, 2H, ArH, J_{HH} = 7.8 Hz), 7.11 (d, CH=CH, 1H, J_{HH} = 16.2 Hz), 6.99 (d, 2H, ArH, J_{HH} = 4.5 Hz), 6.97 (d, 2H, ArH, J_{HH} = 5.9 Hz), 6.73 (d, CH=CH, 1H, J_{HH} = 16.2 Hz), 3.83 (m, 1H, η^2-CH=CH), 3.70 (m, 1H, η^2−CH=CH), 1.23 (m, 12H, PCH_2CH_3), 0.91 (m, 18H, PCH_2CH_3). $^{13}C\{^1H\}$ NMR (acetone-d_6): δ 157.3 (dd, C_q, J_{PtC} = 47.8 Hz, J_{PC} = 5.8 Hz, J_{PC} = 1.6 Hz), 151.9, 150.0, 148.3, 148.2, 145.1 (s, C_q), 133.3, 132.3, 130.7 (C_q, J_{PtC} = 12.2 Hz, J_{PC} = 2.7 Hz), 128.2 (C_q), 127.5, 126.4 (dt, J_{PtC} = 17.6 Hz, J_{PC} = 2.7 Hz), 122.7 (s), 120.7, 120.4, 119.6 (d, J_{PtC} = 17.7 Hz, J_{PC} = 2.4 Hz), 50.6 (dd, η^2-CH=*C*H, J_{PtC} = 207.5 Hz, J_{PC} = 34.1 Hz, J_{PC} = 4.8 Hz), 48.9 (dd, η^2-*C*H=CH, J_{PtC} = 198.0 Hz, J_{PC} = 32.5 Hz, J_{PC} = 5.5 Hz), 19.4 (d of m, PCH_2CH_3, J_{PtC} = 54.0 Hz, J_{PC} = 37.6 Hz, J_{PC} = 23.7 Hz), 7.8 (m, PCH_2CH_3, J_{PtC} = 31.0 Hz, J_{PC} = 16.5 Hz, J_{PC} = 7.2 Hz). $^{31}P\{^1H\}$ NMR (*o*-xylene-d_{10}): δ = 15.5 (AM part of the AMX system, 1P, J_{PP} = 43 Hz, J_{PtP} = 3631.5 Hz), 14.9 (AM part of the AMX system, 1P, $^2J_{PP}$ = 43 Hz, $^1J_{PtP}$ = 3523.2 Hz). $^{195}Pt\{^1H\}$ NMR (C_6H_6): δ −5111.2 (dd, 1Pt, X part of the AMX system, $^1J_{PPt}$ = 3523.6 Hz, $^1J_{PPt}$ = 3631.1 Hz). Calc *m/e*: 715.3, found *m/e*: 715.0. Anal. Calcd for $C_{32}H_{46}N_2P_2Pt$: C, 53.70; H. 6.48. Found: C, 53.57; H, 6.55.

Formation of Complex 3. A solution of $Pt(PEt_3)_4$ (116 mg, 0.174 mmol) in 10 mL of THF was dropwise added to a solution of bis-1,4-(4-pyridylethyl-enyl)-benzene (**1**)[46] (25 mg, 0.087 mmol) in 6 mL of dry THF and stirred at room temperature. $^{31}P\{^1H\}$ NMR spectroscopy of an aliquot indicated the formation of complexes **2** and **3** in a ratio of 3.9:1 after 1 day. All volatiles were removed in vacuo after 1 week in order to remove PEt_3. The residue was redissolved in 4 mL of THF, and the reaction was continued. $^{31}P\{^1H\}$ NMR spectroscopy of an aliquot indicated the formation of complexes **2** and **3** in a ratio of 2.3:1 after 10 days. All volatiles were removed in vacuo after 15 days, and the residue was washed with ~6 mL of dry pentane. Subsequently, the remaining solid was redissolved in 5 mL of THF and stirred for an additional 15 days. The volatiles were again removed, and the residue was redissolved in 1.5 mL of THF. Subsequently, 5 mL of pentane was added, resulting in X-ray quality crystals at −30 °C. ^1H NMR (C_6D_6): δ 8.1 (d, 4H, PyrH, J_{HH} = 4.7 Hz), 6.85 (br, 8H, ArH), 4.25 (m, 4H, CH=CH), 1.57 (m, 24H, PCH_2CH_3), 0.92 (m, 36H, PCH_2CH_3). $^{13}C\{^1H\}$ NMR (C_6D_6): δ 157.7 (d, C_q, J_{PtC} = 48.6 Hz, J_{PC} = 5.1 Hz), 151.9, 148.9, 143.5 (m, br, C_q), 128.2 (d, J_{PtC} = 61.5 Hz, J_{PC} = 3.4 Hz), 124.8 (d, br, J_{PtC} = 66.2 Hz), 119.8, 50.0 (dd, η^2-*C*H=CH, J_{PC} = 31.8 Hz, J_{PC} = 6.2 Hz), 48.9 (dd, η^2-*C*H=CH, J_{PC} = 31.8 Hz, J_{PC} = 6.4 Hz), 20.0 (m, PCH_2CH_3, J_{PtC} = 54.0 Hz, J_{PC} = 37.6 Hz, J_{PC} = 23.7 Hz), 8.10 (dt, PCH_2CH_3, J_{PC} = 23.1 Hz, J_{PC} = 2.4 Hz). $^{31}P\{^1H\}$ NMR (toluene-d_8): δ 16.8 (d, 1P, $^2J_{PP}$ = 45.7 Hz, $^1J_{PtP}$ = 3695.4 Hz), δ 15.4 (d, 1P, $^2J_{PP}$ = 48.0 Hz, $^1J_{PtP}$ = 3459.7 Hz) $^{195}Pt\{^1H\}$ NMR (C_6H_6, 107.04 MHz): δ −5072.3 (ddd, 2Pt, $^1J_{PPt}$ = 3696.1 Hz, $^1J_{PPt}$ = 3458.2 Hz). Anal. Calcd for $C_{44}H_{76}N_2P_4Pt_2$: C, 46.07; H. 6.68. Found: C, 46.07; H, 6.32.

Formation of Complex 3 from Complex 2 and $Pt(PEt_3)_4$. A solution of $Pt(PEt_3)_4$ (66.7 mg, 0.100 mmol) in 8 mL of THF was added dropwise to a solution of complex **2** (66 mg, 0.092 mmol) in 6 mL of dry THF and stirred at room temperature. $^{31}P\{^1H\}$ NMR spectroscopy of an aliquot indicated the presence of complexes **2** and **3** in a ratio of 1:1 after 1 day. All volatiles were removed in vacuo after 3 days in order to remove PEt_3, and the residue was redissolved in 4 mL of THF. $^{31}P\{^1H\}$ NMR spectroscopy of an aliquot indicated the formation of complexes **2** and **3** in a ratio of 1:4 after 8 days. The reaction was completed in 27 days, and complex **3** was isolated in good yield (82%) by washing with 1.5 mL of cold (−30 °C) pentane.

X-ray Analysis of Complex 3. Crystal Data. $^1/_2(C_{44}H_{76}N_2P_4Pt_2)$, yellow, prism, 0.2 × 0.2 × 0.2 mm^3, triclinic, $P\bar{1}$ (No. 2), a = 9.150(2) Å, b = 10.656(2) Å, c = 13.211(3) Å, α = 76.63(3)°, β = 79.76(3)°, γ = 79.10(3)°, T = 120(2) K, V = 1218.4(4) Å^3, Z = 1, Fw = 571.55, Dc = 1.558 Mg m^{-3}, μ = 5.896 mm^{-1}.

Data Collection and Processing. Nonius KappaCCD diffractometer, Mo Kα (λ = 0.71073 Å), graphite monochromator, −11 ≤ h ≤ 11, −13 ≤ k ≤ 13, 0 ≤ l ≤ 17, frame scan width = 2°, scan speed 1.0° per 40 s, typical peak mosaicity 0.43°, 23018 reflections collected, 5530 independent reflections (R-int = 0.066). The data were processed with Denzo-Scalepack.

Solution and Refinement. The structure was solved by the Patterson method with SHELXS-97.[50] The full matrix least-squares refinement is based on F^2 with SHELXL-97 235 parameters with 2 restraints, final R_1 = 0.034 (based on F^2) for data with $I > 2\sigma(I)$

(46) Detert, H.; Stalmach, U.; Sugiono, E. *Synt. Met.* **2004**, *147*, 227.
(47) Schunn, R. A. *Inorg. Chem.* **1976**, *15*, 208.
(48) Amorso, A. J.; Cargill Thompson, A. M. W.; Mahes, J. P.; McCleverty, J. A.; Ward, M. W. *Inorg. Chem.* **1995**, *34*, 4828.
(49) Vatsadze, S. Z.; Nuriev, V. N.; Chernikov, A. V.; Zyk, N. V. *Russ. Chem. Bull.* **2002**, *51*, 1957.
(50) Sheldrick, G. M. *SHELXL-97: Program for Crystal Structure Determination*; University of Göttingen: Göttingen, Germany, 1997.

and $R_1 = 0.049$ on 5525 reflections, goodness-of-fit on $F^2 = 1.041$, largest electron density peak = 2.991e.Å^{-3}.

Formation of Complex 5. A solution of $Pt(PEt_3)_4$ (23 mg, 0.034 mmol) in 3 mL of THF was dropwise added to a solution of *trans*,*trans*-9,10-bis(4-pyridylethenyl)anthracene (**4**)[46] (13 mg, 0.034 mmol) in 5 mL of dry THF and stirred at room temperature for 15 min. Removal of all volatiles in vacuo and washing of the residue with ~6 mL of dry pentane afforded the analytically pure complex **5** as an orange solid in 83% yield. ^{1}H NMR (C_6D_6): δ 9.38 (br, 2H, PyrH), 8.68–8.48 (q, AB system, 4H, J_{HH} = 4.9 Hz, ArH), 8.39–8.33 (m, PyH, 2H, J_{HH} = 8.9 Hz), 7.83 (dd, CH=CH, 1H, J_{HH} = 16.5 Hz), 7.3 (br, 4H, PyrH), 6.9 (m, br, 4H, ArH, J_{HH} = 5.3 Hz), 6.5 (dd, CH=CH, 1H, J_{HH} = 16.5 Hz), 5.59 (m, 1H, CH=CH, J_{PtH} = 53.5 Hz), 4.05 (m, 1H, CH=CH, J_{PtH} = 41.9 Hz), 1.42–1.14 (d of m, 12H, PCH_2CH$_3$), 0.93–0.65 (d of m, 18H, PCH$_2$CH_3). ^{13}C{^{1}H} NMR (C_6D_6): δ 158.5 (dt, C_q, J_{PtC} = 44.3 Hz), 151.8, 150.6, 149.3, 144.1 (s, C_q), 143.6 (s, C_q), 135.5, 134.6, 132.5, 130.5, 130.3 (s, C_q), 129.4 (s, C_q), 128.0, 126.8, 126.4, 125.8, 124.9, 123.9 (br), 120.7, 120.6, 119.77 (s, J_{PtC} = 16.1 Hz), 54.0 (dd, η^2-CH=*C*H, J_{PtC} = 230.3 Hz, J_{PC} = 31.7 Hz, J_{PC} = 4.3 Hz), 46.9 (dd, η^2-*C*H=CH, J_{PtC} = 215.0 Hz, J_{PC} = 31.7 Hz, J_{PC} = 2.8 Hz), 20.3 (doublet of m, P*C*H$_2$CH$_3$, J_{PtC} = 63.6 Hz, J_{PC} = 23.2 Hz, J_{PC} = 3.1 Hz), 8.11 (m, PCH$_2$*C*H$_3$, J_{PtC} = 23.3, J_{PC} = 17.9 Hz). ^{31}P{^{1}H} NMR (C_6D_6): δ 15.2 (AM part of the AMX system, 1P, $^2J_{PP}$ = 40.9 Hz, $^1J_{PtP}$ = 3590.6 Hz), 14.9 (AM part of the AMX system, 1P, $^2J_{PP}$ = 40.9 Hz, $^1J_{PtP}$ = 3540.3 Hz. ^{195}Pt{^{1}H} NMR (C_6D_6, 107.04 MHz): δ −5067.2 (dd, 1Pt, X part of the AMX system, $^1J_{PPt}$ = 3590.0 Hz, $^1J_{PPt}$ = 3540.4 Hz). Calcd *m*/*e*, 815.8; found *m*/*e*, (M + 1) = 817.2: Anal. Calcd for $C_{40}H_{50}N_2P_2Pt$: C, 58.89; H. 6.18, N, 3.43. Found: C, 58.15; H. 6.25, N, 3.16.

Variable Temperature (VT) ^{1}H NMR Experiments with Complexes 2 and 5. A solution of complex **2** (25 mg, 0.035 mmol) in 1 mL of *o*-xylene-d_{10} was loaded in a 5-mm screw-cap NMR tube that was sealed using Teflon tape and parafilm. The temperature dependence was followed by ^{1}H and ^{31}P{^{1}H} NMR spectroscopy in the range of −90 to 120 °C. The room temperature ^{1}H NMR spectrum of complex **2** shows well-resolved signals for all protons of complex **2**, and upon increasing the temperature, all the signals start to broaden. The process is reversible. The ^{31}P{^{1}H} NMR spectra shows some broadening at higher temperatures. No uncomplexed ligand (**1**) and $Pt(PEt_3)_x$ (x = 2–4) were observed. The ^{1}H NMR spectrum is not affected by cooling the sample to −90 °C. No concentration effects were observed within the range of 0.0035–0.035 mmol/mL for complex **2** in *o*-xylene-d_{10}. Performing the VT experiments in the presence of PEt_3 (2 equiv) did not affect the spectra. VT ^{1}H NMR spectroscopy was performed with complex **5** within the range of 35−110 °C in *o*-xylene-d_{10}. No concentration effects were observed when comparing samples containing 0.0078 mmol/mL versus 0.0306 mmol/mL of complex **5**. Performing the VT experiment with 0.0306 mmol/mL of complex **5** in the presence of PEt_3 (2 equiv) resulted in the formation of uncomplexed ligand **4** and $Pt(PEt_3)_3$.

Spin Saturation Transfer (SST) Measurements: Determination of Activation Parameters. In a typical experiment, a 5-mm screwcap NMR tube with a *o*-xylene-d_{10} solution of complex **2** (0.0279 mmol/mL) was placed in a Bruker Avance 500 NMR instrument. SST experiments were performed by selective saturation of the signal at δ ~ 3.8 ppm, corresponding to the olefinic protons of the C=C moiety η^2-coordinated to the metal center. The response of the signals of the "free" olefinic protons at δ 7.11 and 6.73 ppm was identified by comparison with control experiments. All measurements were repeated at least 2 times. The relaxation rate (R_{obs}) of the olefinic proton at δ 7.11 ppm was measured using the standard inversion–recovery technique, combined with the saturation of the target peak resonance (the signal of the other olefinic proton at δ 6.73 ppm was partially overlapped with a peak of the solvent). The rate constants, k_{obs}, were calculated using the Forsen−Hoffman equation: $M^\infty/M^c = R_B/(R_B + k_{obs})$, where $R_{obs} = R_B + k_{obs}$ and M^∞ is the area of the signal at δ 7.11 ppm during saturation of the target resonance at δ 3.8 ppm, and M^c is the signal intensity of the control experiment.[51,52] Similar SST experiments were performed with complex **5** (0.0245 mmol/mL; *o*-xylene-d_{10}). SST experiments were performed within the range 35–60 °C by selective saturation of the signals at δ 5.59 and 4.05 ppm, corresponding to the olefinic protons of the −C=C− moiety η^2-coordinated to the metal center. The response of the signals of the "free" olefinic protons at δ 7.83 and 6.5 ppm was identified by comparison with control experiments. The responses are quantitative at 60 °C.

Spin Saturation Transfer Measurements: Competition Experiments. In a representative experiment, an NMR sample containing a mixture of complex **2** (5.5 mM) and ligand **1** (2.25 mM) in C_6D_6 was used. SST experiments were performed by preirradiation of desired resonances utilizing irradiation powers sufficient to completely annihilate the target peaks. For instance, the multiplet at δ ~3.8 ppm, corresponding to the olefinic protons of the C=C− moiety η^2-coordinated to the metal center, was chosen as the target signal. Subsequently, the responses were verified by comparison with control experiments, which include irradiation of signal-free areas under the same conditions. At room temperature, preirradiation of the olefinic protons results only in a positive NOE response of the adjacent aromatic protons of complex **2** owing to the closeness in space. At 40–47 °C, preirradiation of the olefinic protons of the C=C moiety η^2-coordinated to the metal center yields quantitative spin saturation transfer (negative response and an intensity decrease) to the "free" olefinic protons as well as positive NOE responses of the aromatic protons of complex **2**. The free ligand's (**1**) olefinic proton resonances remained unchanged with respect to the control experiments. VT SST competition experiments between complex **5** and ligand **4** were also performed; however, there is overlap of signals. Preirradiation of the protons of the η^2-C=C moiety of complex **5** (δ 4.05 ppm and at δ = 5.59 ppm) at 45 °C yields spin saturation transfer (160%) to the protons of the C=C groups of complex **5** and ligand **4** (these signals are overlapped). Performing this experiment with complex **5** results in a much smaller response (40%) under identical conditions.

Results and Discussion

Reaction of an equimolar amount of $Pt(PEt_3)_4$ with bis-1,4-(4-pyridylethyl-enyl)-benzene (**1**)[46] in dry THF at room temperature for ~10 min resulted in the quantitative formation of complex **2** (Scheme 3). Complex **2** was formed quantitatively, as judged by ^{31}P{^{1}H} NMR spectroscopy, isolated (85%), and was characterized by combining ^{1}H, ^{13}C{^{1}H}, ^{31}P{^{1}H}, and ^{195}Pt{^{1}H} NMR spectroscopy, elemental analysis, and mass spectrometry. Assignment of the ^{1}H and ^{13}C{^{1}H} NMR spectra was made using COSY and ^{13}C-DEPT135 NMR spectroscopy. Coordination of the metal center to one of the C=C bonds resulted in an unsymmetrical system, as revealed by ^{1}H and ^{13}C{^{1}H} NMR spectroscopy. An AMX spin system was observed by ^{31}P{^{1}H} and

(51) Lian, L.-Y.; Roberts, G. C. K. *NMR of macromolecules, The practical approach*; IRL Press: Oxford, 1993.
(52) Forsen, S.; Hoffman, R. A. *J. Chem. Phys.* **1964**, *40*, 1189.

Scheme 3. Selective Formation of Complexes **2** and **3** by η^2-Coordination of $Pt(PEt_3)_2$ to the C=C Bonds of Ligand **1**

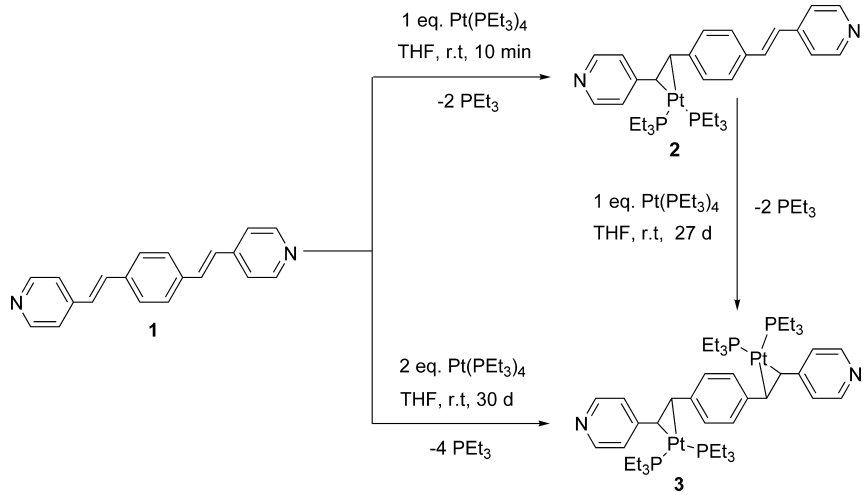

$^{195}Pt\{^1H\}$ NMR spectroscopy. In the $^{31}P\{^1H\}$ NMR spectrum, the AM part appears at $\delta \sim 15$ ppm as a quartet with $^2J_{PP(cis)} = 43$ Hz, flanked by platinum satellites ($^1J_{PtP} \approx 3500$ Hz). In the $^{195}Pt\{^1H\}$ NMR spectrum, the X part of the AMX system appears as a double doublet at δ −5111.2 with $^1J_{PtP} = 3500$–3600 Hz. The η^2-coordination of the metal center to one of the C=C moieties is apparent from the ^1H and $^{13}C\{^1H\}$ NMR spectra, which exhibit signals typical for such interactions at δ 3.8 and at δ 50.6 ppm, respectively. The two carbon atoms of the η^2-C=C moiety are inequivalent and are coupled with ^{195}Pt and with both *cis* and *trans* PEt_3 ligands.

Reaction of complex **2** with an equimolar amount of $Pt(PEt_3)_4$ or reaction of ligand **1** with two equivalents of $Pt(PEt_3)_4$ resulted in the selective formation of the bimetallic complex **3** after 27 days (Scheme 3). The reaction was stopped several times to remove released phosphine to drive the reaction to completion. Apparently, coordination of the second metal center to complex **2** is more than 3 orders of magnitude slower in comparison with the formation of the monometallic system (**2**). The rather sluggish reactivity of complex **2** with $Pt(PEt_3)_4$ is probably due to steric hindrance because the ^1H and $^{31}P\{^1H\}$ NMR data of complex **2** indicate that the nature of the "free" C=C unit is not affected by binding of the metal center to the ligand system (**1**). Attempts to form complex **3** at higher temperatures (e.g., 80 °C) did not appreciably improve the reaction time. Complex **3** was fully characterized by combining ^1H, $^{13}C\{^1H\}$, $^{31}P\{^1H\}$, and $^{195}Pt\{^1H\}$ NMR spectroscopy, elemental analysis, mass spectrometry, and by single-crystal X-ray crystallography.

The X-ray analysis unambiguously confirms the bimetallic nature of complex **3**, having the metal centers η^2-coordinated to the two C=C bonds of ligand **1** in *trans* position (Figure 1) The coordination of the platinum moieties induces significant lengthening of the C=C bonds (i.e., C(6)−C(7) = 1.467 Å) in comparison with those of the ligand (**1**) (1.327Å).[53] Complex **3** exhibits a nearly planar geometry around the metal centers. Each metal center is in a plane containing a C=C bond and the PEt_3 ligands, with angles of P(1)−Pt(1)−P(2) = 103.84° and C(6)−Pt(1)−C(7) = 40.26°. These characteristic features are typical for Pt(0)-olefin complexes.[4] A common plane between the three aromatic rings is not observed. Instead, the two pyridyl groups are twisted in opposite directions with respect to the plane of the central aromatic ring. The angle between each pyridyl group and the central aromatic ring is 41.36°. This conformation is most likely due to the steric hindrance of the ethyl groups. Apparently, some electron delocalization takes place at the expense of aromaticity of the pyridine units and the central aromatic rings. For example, the structural data shows that C(2)−C(3), C(4)−C(5), and C(9)−C(12) become localized double bonds at 1.392(8), 1.370(7), and 1.377(7) Å, respectively. Whereas the C(1)−C(2), C(1)−C(5),

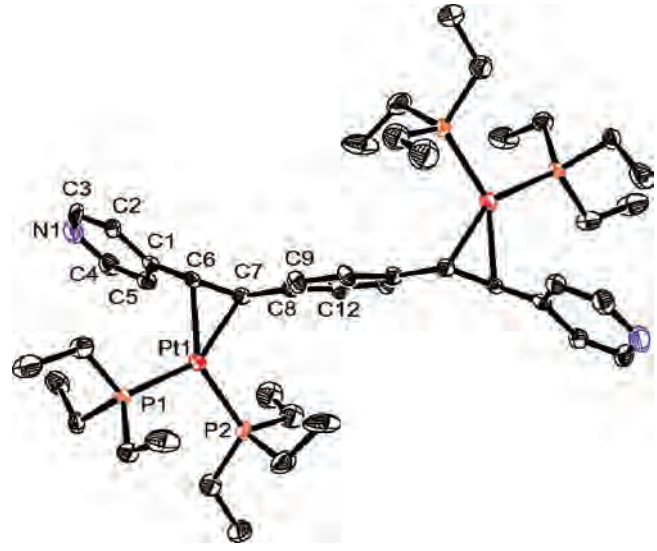

Figure 1. ORTEP diagram of complex **3** with thermal ellipsoids set at 50%, probability showing the η^2-coordination of the two $Pt(PEt_3)_2$ groups to the C=C bonds. There is $^1/_2$ molecule of complex **3** per asymmetric unit. Hydrogen atoms are omitted for clarity. Selected bond length (Å) and angles (°): Pt(1)−C(7) 2.129(4), Pt(1)−C(6) 2.131(5), Pt(1)−P(2) 2.2664(13), Pt(1)−P(1) 2.2754(14), C(1)−C(2) 1.415(6), C(2)−C(3) 1.392(8), C(1)−C(5) 1.412(7), C(4)−C(5) 1.370(7), C(1)−C(6) 1.468(7), C(6)−C(7) 1.467(6), C(7)−C(8) 1.477(6), C(8)−C(9) 1.403(6), C(9)−C(12) 1.377(7), C(8)−C(12) 1.414(6), C(6)−Pt(1)−C(7) 40.28(16), C(7)−Pt(1)−P(2) 106.86(12), C(6)−Pt(1)−P(2) 147.12(12), C(7)−Pt(1)−P(1) 109.03(12), P(1)−Pt(1)−P(2) 103.84(5).

(53) Friscic, T.; MacGillivray, L. R. *Chem. Commun.* **2003**, 1306.

Scheme 4. Migration of the $Pt(PEt_3)_2$ Moeity of Complex **2** between the two C=C Bonds of Ligand **1** at Elevated Temperatures

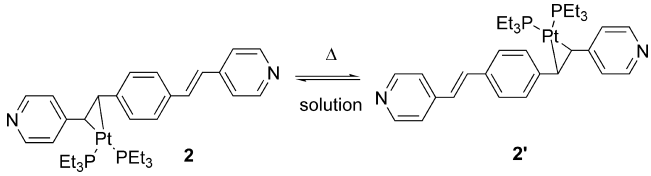

and C(8)−C(12) bonds are relatively long (1.415(6), 1.412(7), 1.414(6) Å, respectively). The C−C bond lengths of the aromatic rings of the free ligand (**1**)[53] all fall within the range of 1.373–1.395 Å. They have some localized character, but they are still clearly primarily aromatic. As expected, the π-backdonation from the d orbitals of the electron-rich Pt centers to the π^* antibonding orbitals of the C=C bonds results in weakening and hence bond lengthening. This also affects the C(1)−C(6) and C(7)−C(8) bond lengths (1.468(7) and 1.477(6) Å, respectively) in comparison with those of the uncomplexed ligand **1**.[53]

VT ^{1}H NMR spectroscopy studies were performed in *o*-xylene-d_{10} to evaluate the dynamic behavior of complex **2**. At room temperature, the ^{1}H NMR spectrum of complex **2** shows relatively sharp resonances that broaden at elevated temperatures. At temperatures above 100 °C, coalescence of some signals is observed. Apparently, the system reaches near-fast exchange at higher temperatures, suggesting a process in which the metal center migrates between the two C=C bonds (**2** ⇄ **2′**), as shown in Scheme 4.

Regardless of the exact nature of this fluxional process, upon cooling, the original ^{1}H NMR spectrum of complex **2** is again observed. Extraction of detailed kinetic information from band shape analysis requires the NMR spectra to be acquired under slow, intermediate, and fast chemical exchange conditions. However, it was not possible to reach the high temperatures (>120 °C) necessary for fast exchange conditions because of the experimental limitation imposed by the NMR instrumentation. Varying the concentration of complex **2** (2.5–25 mg/mL) does not affect the VT NMR spectra, indicating that the overall process is first order in complex **2** (Figure 2). Performing the VT NMR experiments in the presence of 2 equiv of PEt_3 also did not affect the system, which might indicate an intramolecular process. In any case, the slow formation of complex **3** makes it highly unlikely that bimetallic complexes are involved (Scheme 3).

Phase-sensitive 2D ^{1}H−^{1}H EXSY VT NMR measurements were carried out to verify that the metal center migrates between the two C=C bonds at elevated temperatures. This experiment, using a phase-sensitive NOESY pulse sequence, provides a visual map of the exchange matrix under conditions of slow exchange (Figure 3). Positive cross-peaks between the protons of the two C=C bonds were observed in the temperature range of 50–90 °C and are in agreement with a metal migration process between these two moieties.

SST experiments were performed with complex **2** within the temperature range of 35–80 °C to determine the activation parameters. A negative response for the "free" C=C bond was observed by selective saturation of the protons of the C=C bond η^2-coordinated to the metal center. The negative

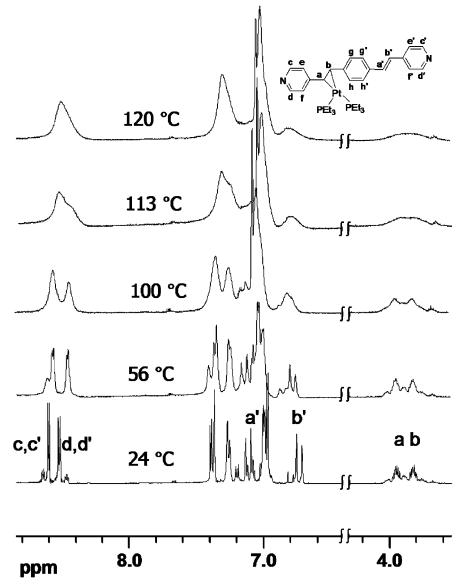

Figure 2. VT ^{1}H NMR spectra of complex **2** (25 mg/mL) in *o*-xylene-d_{10}.

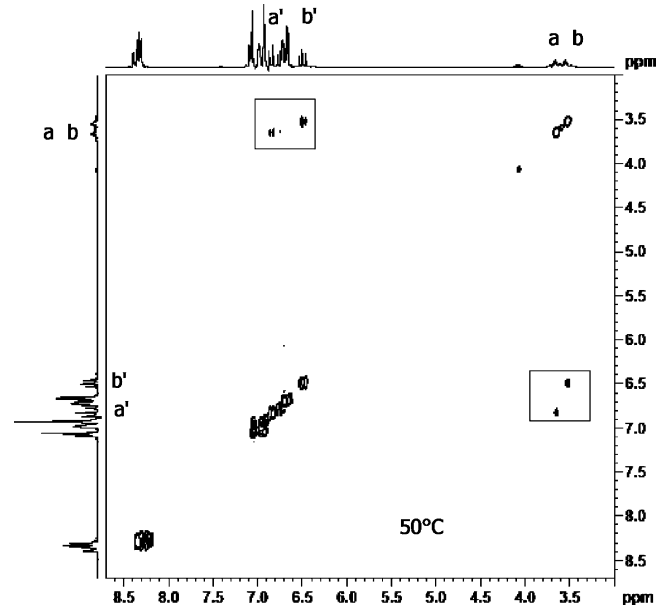

Figure 3. VT ^{1}H−^{1}H EXSY NMR spectrum of complex **2** in toluene-d_8 at 50 °C showing exchange cross-peaks, demonstrating that both the C=C moieties are involved in chemical exchange processes. The cross-peaks are more intense at 90 °C, whereas at room temperature no correlations were observed.

response increases as the temperature increases. The rate constants, k_{obs}, were calculated by means of the Forsen−Hoffman equation.[51,52] Repeat measurements yielded almost identical values. The activation parameters, $\Delta H^{\ddagger} = 21.9 \pm 1.2$ kcal/mol, $\Delta S^{\ddagger} = 6.4 \pm 2.5$ e.u., and $\Delta G^{\ddagger} = 19.4 \pm 1.2$ kcal/mol, for the rearrangement **2** ⇄ **2′** were derived from the Eyring plot shown in Figure 4.

Mechanistically, the transformation of **2** ⇄ **2′** may proceed via rapid $Pt(PEt_3)_2$ dissociation/association at elevated temperatures. Alternatively, the process may involve an intramolecular metal ring-walking process. The low entropy values, $\Delta S^{\ddagger}$, indicate that neither metal–ligand dissociation nor metal–ligand association type process exists at the rate determining step (otherwise a large positive or negative

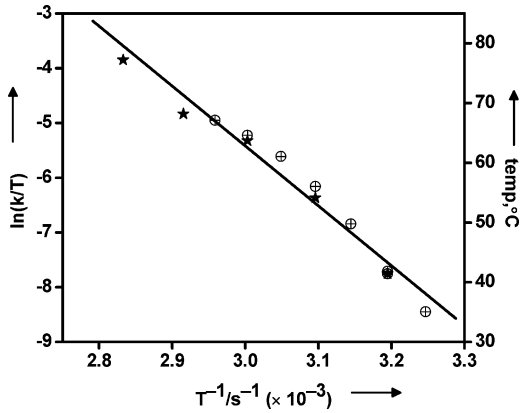

Figure 4. Eyring plot of the conversion of **2** ⇄ **2′** ($R^2 = 0.984$) in *o*-xylene-d_{10} (27.9 mM). ⊕ and ★ correspond to two series of independent measurements of different samples of complex **2**.

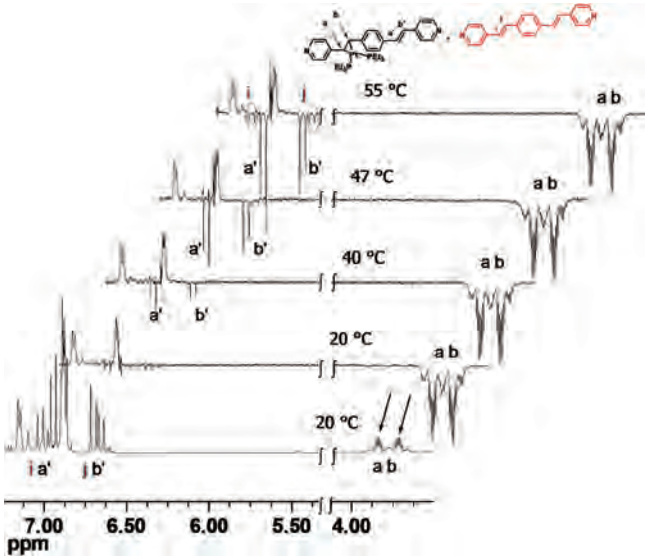

Figure 5. VT Spin Saturation transfer experiments with complex **2** in the presence of 0.5 equiv of ligand **1** in C_6D_6. The lower spectrum shows the ^{1}H NMR spectrum at δ 7.24–3.5 ppm. The arrows indicate the irradiated peaks (a, b). The four upper spectra recorded in the range of 20–55 °C are difference spectra between that with irradiation of the signal at δ 3.8 ppm and the normal spectrum.

value, respectively, would be expected). The entropy, being small, is consistent with either (i) an intramolecular process or (ii) metal–ligand dissociation that is not the rate determining step. A process involving rate-limiting metal dissociation would have larger positive entropy. Apparently, the transformation of **2** ⇄ **2′** is intramolecular. In order to provide support for this hypothesis, we used VT SST measurements of complex **2** in the presence of free ligand **1**. For this experiment, a 2:1 mixture of complex **2** and free ligand **1** was used. It was found that the magnetization transfer occurred exclusively within complex **2**, as expected for an intramolecular rearrangement.[10,21–23] No intermolecular magnetization transfer to the free ligand (**1**) was observed within the temperature range of 25–47 °C. A stack plot of a typical magnetization transfer experiment is shown in Figure 5. At 55 °C, ~17% of the magnetization was transferred to the ligand (**1**) and 83% of the magnetization was still transferred within complex **2**, indicating the presence of some ligand scrambling in parallel to an intramolecular process at higher

Scheme 5. Selective Formation of Complex **5** and Migration of the $Pt(PEt_3)_2$ Moeity of Complex **5** between the two C=C Bonds of Ligand **4** at Elevated Temperatures

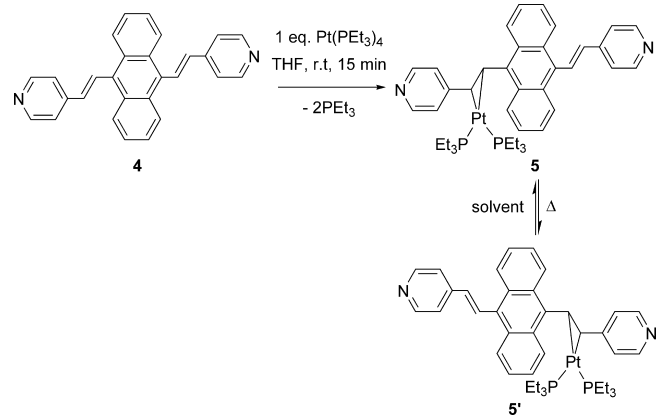

temperatures. The process of this ligand exchange is not straightforward: $Pt(PEt_3)_2$ dissociation is probably not occurring because of the relatively low $\Delta S^{\ddagger}$ values and the linear correlation observed for k_{obs} versus temperature (at least up to 80 °C; Figure 4). Alternatively, an associative ligand exchange process of ligand **1** with metal complex **2** may account for the observed magnetization transfer at higher temperatures.

Complex **5** was prepared in order to evaluate the role of the central aromatic system on the metal migration process (Scheme 5). Reaction of an equimolar amount of $Pt(PEt_3)_4$ with *trans*,*trans*-9,10-bis(4-pyridylethenyl)anthracene (**4**)[54] in dry THF at room temperature for 20 min led to the quantitative formation of complex **5**. Complex **5** was isolated and fully characterized in the same way as complex **2**.

The X-ray structure of compound **4** shows that the anthracene and the vinylpyridine moieties are not in the same plane,[54] probably because of steric hindrance between the olefinic and aromatic protons. The barrier to becoming coplanar is probably quite low in the free ligand (**4**). However, the $Pt(PEt_{3)})_2$ group of complex **5** may induce a larger barrier for the π-system to become coplanar. In such a case, it is less likely for the metal center to use the aromatic system as a pathway to migrate to the other C=C bond. As for complex **2**, VT ^{1}H NMR spectroscopy in the range of 35–110 °C shows (reversible) broadening of the signals with increasing temperature. The concentration of complex **5** does not affect the VT NMR spectra indicating that the overall process is first order (unimolecular) in complex **2**. Stanger has shown that if the rate determining step is unimolecular, and depends only on the complex,[10,21–23] one can not distinguish between a ring-walking and a dissociative process by varying the concentration (Scheme 1, **I** ⇄ **I′**). Performing the VT NMR experiments in the presence of 2 equiv of PEt_3 resulted in formation of $Pt(PEt_3)_3$ and uncomplexed ligand **4**. VT ^{1}H−^{1}H EXSY NMR spectroscopy showed exchange cross peaks at 40 °C between the signals of the C=C moieties (δ 5.59–4.05 and 7.83–6.5 ppm). Apparently, the platinum center of complex **5** migrates between the C=C bonds of

(54) Sokolov, T. N.; Friscic, T.; MacGillivray, L. R. *J. Struct. Chem.* **2005**, *46*, S171.

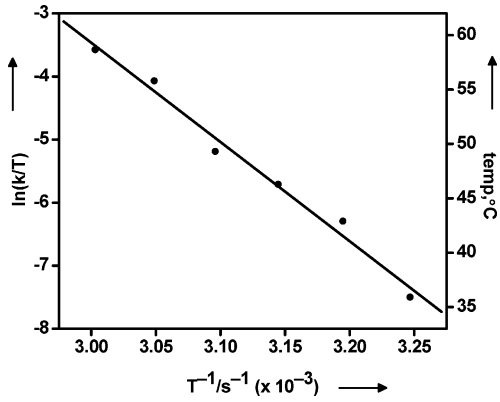

Figure 6. Eyring plot of the conversion of **5** ⇄ **5′** ($R^2 = 0.985$) in *o*-xylene-d_{10} (24.5 mM).

ligand **4**. From the above mentioned observations, it is not clear whether inter or intramolecular pathways are involved. The observed metal–ligand dissociation due to the addition of PEt_3 might be explained as follows: (i) The PEt_3 reacts with complex **5** to afford the observed free ligand (**4**) and $Pt(PEt_3)_3$, or (ii) complex **5** is in (an unobserved) equilibrium with ligand (**4**) and $Pt(PEt_3)_2$; addition of PEt_3 shifts this equilibrium toward the observed ligand **4** and $Pt(PEt_3)_3$. In any case, the metal center in complex **5** seems less strongly bound to the ligand than in complex **2**. Competition experiments between complex **5** and ligand **4** were difficult to monitor by VT SST experiments because of the overlap of the signals. Regardless of these limitations, it is possible to observe intermolecular magnetization transfer to the free ligand (**4**) at 45 °C by comparison between SST experiments with and without added ligand (**4**). The magnetization transfer between the protons of the C=C groups increases 4-fold upon addition of an equimolar amount of ligand to a solution of complex **5**. However, these observations do not exclude a ring-walking process.

We used SST NMR experiments at various temperatures (ranging from 35 to 60 °C) to gain more insight into the fluxional behavior of complex **5**. The activation parameters for the rearrangement **5** ⇄ **5′**, $\Delta H^{\ddagger} = 31.3 \pm 1.9$ kcal/mol, $\Delta S^{\ddagger} = 39.7 \pm 6.0$, and $\Delta G^{\ddagger} = 19.5 \pm 1.9$ kcal/mol were derived from an Eyring plot (Figure 6). Interestingly, both the $\Delta H^{\ddagger}$ and $\Delta S^{\ddagger}$ values are much larger than observed for complex **2** (under identical reaction conditions). The large differences in the activation parameters between systems **2** and **5** may support the notion of different mechanistic pathways. The large positive entropy value suggests that an intermolecular process operates for the migration of the metal center in complex **5**. Replacing the central ring system of ligand **1** with the larger anthracene group (**4**) may induce significant steric hindrance, thus effectively weakening the platinum−ligand bond and blocking the $Pt(PEt_3)_2$ moiety from "ring walking". It is known that the intra versus the intermolecular migration of a $(R_3P)_2Ni$ (R = Et, Bu) moiety over anthracene ligands (Scheme 1, **I** ⇄ **I′**) is controlled by substituents attached to the arene.[21]

Summary and Conclusions

A chemical exchange process in which a platinum moiety migrates between two C=C bonds bridged by an arene has been observed for complexes **2** and **5**. VT SST NMR experiments unambiguously showed that the metal migration between the two C=C bonds of the metal complex **2** is intramolecular, even in the presence of free ligand **1**. In support of the unimolecular route: no magnetization transfer was observed to ligand **1** at temperatures below 47 °C. SST is a powerful method for determining the intra versus intermolecular nature of dynamic processes. For instance, it has been used to study the fluxional behavior of nickel−anthracene systems such as **I** (Scheme 1).[10,21,23] The low entropy value for **2** ⇄ **2′**, $\Delta S^{\ddagger} = 6.4 \pm 2.5$ e.u., also supports the existence of an intramolecular process. A reasonable mechanistic scenario for the intraconversion of **2** ⇄ **2′** is a series of intramolecular haptotropic rearrangements. Several organometallic systems are known to undergo "ring walking"; however, reversible metal migration between a C=C moiety and an arene is rare.[30] The mechanistic information for complex **5** is mainly based on the activation parameters derived by SST, with a relative small temperature range (ΔT = 25 °C). However, the difference between the entropy values of the two systems is larger than 33 e.u. The relative large, positive entropy value for **5** ⇄ **5′**, $\Delta S^{\ddagger} = 39.7 \pm 6.0$ e.u., supports the existence of an intermolecular pathway. This is in agreement with the observed metal–ligand dissociation at elevated temperatures in the presence of PEt_3, and the significant magnetization transfer to ligand **4**.

The ease by which the metal center migrates between different molecular moieties of system **2** via an intramolecular pathway may suggest that some organometallic transformations involving arene and olefinic substrates may involve similar routes. The introduction of dynamic, loosely bound metal-based moieties into rigid, well-defined systems through η^2-complexation could lead to new supramolecular structures with tailorable properties.

Acknowledgment. This research was supported by the Helen and Martin Kimmel Center for Molecular Design and the German-Israel Foundation (GIF). M.E.vd.B. is the incumbent of the Dewey David Stone and Harry Levine Career Development Chair.

Supporting Information Available: Crystallographic data (CIF) for complex **3**. This material is available free of charge via the Internet at http://pubs.acs.org.

IC702433S